Global cropland nitrous oxide emissions in fallow period are comparable to growing-season emissions

Ziyin Shang[1#], Xiaoqing Cui[2#], Kees Jan van Groenigen[3], Matthias Kuhnert[4], Mohamed Abdalla[4], Jiafa Luo[5], Weijian Zhang[1], Zhenwei Song[1], Yu Jiang[6], Pete Smith[4], Feng Zhou[7, 8*]

ORCID iDs: Ziyin Shang: https://orcid.org/0000-0001-8840-0380; Xiaoqing Cui: https://orcid.org/0000-0002-1970-5145; Kees Jan van Groenigen: https://orcid.org/0000-0002-9165-3925; Matthias Kuhnert: https://orcid.org/0000-0003-3284-2133; Mohamed Abdalla: https://orcid.org/0000-0001-8403-327X; Jiafa Luo: https://orcid.org/0000-0001-6198-6887; Weijian Zhang: https://orcid.org/0009-0006-9043-687X; Zhenwei Song: https://orcid.org/0000-0001-9057-2157; Yu Jiang: https://orcid.org/0000-0002-4241-1858; Pete Smith: https://orcid.org/0000-0002-3784-1124; Feng Zhou: https://orcid.org/0000-0001-6122-0611

[1] Institute of Crop Sciences, Chinese Academy of Agricultural Sciences, Beijing 100081, China

[2] School of Grassland Science, Beijing Forestry University, Beijing, China

[3] Department of Geography, College of Life and Environmental Sciences, University of Exeter, Exeter, UK

[4] Institute of Biological and Environmental Sciences, University of Aberdeen, 23 St Machar Drive, Aberdeen AB24 3UU, UK

[5] AgResearch Ruakura, Hamilton, 3240, New Zealand

[6] College of Agronomy, Nanjing Agricultural University, Nanjing, China

[7] Laboratory for Earth Surface Processes, College of Urban and Environmental Sciences, Peking University, Beijing 100871, P.R. China

[8] College of Geography and Remote Sensing, Hohai University, Nanjing, China

[#] Ziyin Shang and Xiaoqing Cui should be considered joint first author.

*** Corresponding author:** Feng Zhou. E-mail: zhouf@pku.edu.cn

Telephone: +8613810171339.

Running Title: Important global fallow-period N_2O emissions

Abstract

Croplands account for ~1/3 of global anthropogenic nitrous oxide (N_2O) emissions. A number of recent field experiments found substantial fallow-period N_2O emissions, which have been neglected for decades. However, the global contribution of the fallow-period emissions and the associated drivers remain unclear. Based on 360 observations across global agroecosystems, we simulated the ratio of the fallow to the whole-year N_2O emissions (R_{fallow}) by developing a mixed-effect model and compiling cropping-system-specific input data. Our results revealed that the mean global gridded R_{fallow} was 44% (15–75%, 95% confidence interval), with hotspots mainly in the northern high latitudes. For most cropping systems, soil pH was the dominant driver of global variation in R_{fallow}. Global cropland emission factors (i.e., the percentage of fertilizer N emitted as N_2O, EFs) in EF-based models doubled to 1.9% when the fallow-period N_2O emissions were included in our simulation, similar to EFs estimated by process-based and atmospheric inversion models (1.8–2.3%). Overall, our study highlights the importance of fallow-period N_2O emissions in annual totals, especially for single cropping systems and croplands in acidic areas. To accurately estimate N_2O emissions for national greenhouse gas inventories, it is crucial to update current EFs with full consideration of the fallow-period N_2O emissions in the Intergovernmental Panel on Climate Change (IPCC) Tier 1 method.

Keywords: nitrous oxide, greenhouse gas, non-growing season, spatial variation, cropping system, simulation, inventory

1 Introduction

N_2O is one of the major agricultural greenhouse gases (GHGs) and the most significant atmospheric ozone-depleting substance (Ravishankara et al., 2009). Most countries in the world are requested by the United Nations Framework Convention on Climate Change (UNFCCC) to compile and report their national GHG and N_2O inventories (Deng et al., 2022). About one-third of anthropogenic N_2O emissions are derived from croplands (Tian et al., 2020). Cropland N_2O emissions are mainly from microbial processes in soils (Butterbach-Bahl et al., 2013), such as nitrification and denitrification, contributing to N loss from the management-driven climate-soil-crop systems. Management practices, such as N fertilizer inputs, cropping period and cropping system selection, play important roles in the cropland N_2O emissions (Cui et al., 2021). Therefore, accurate estimates of regional cropland N_2O emissions are crucial for developing and adjusting agricultural management strategies aimed at mitigating both climate change and ozone depletion.

Cropland N_2O emission can be estimated through different methodologies (e.g., EF-based, atmospheric inversion, and process-based models) with large discrepancies. One potential factor for the underestimation of N_2O emissions in GHG inventories is the omission of emissions during fallow (non-growing) periods (Shang et al., 2020). Most N_2O emission fluxes used for building the EF-based inventories are measured during growing seasons rather than whole years (Cui et al., 2021; Shang et al., 2020), since the fallow periods usually come with cold weather and limited residual N. However, field observations suggest that fallow-period N_2O emissions accounted for 36% on average of the annual emissions for wheat and maize in Canada (Ekwunife et al., 2022; Pelster et al., 2022), and even more for rice paddies in Asia. Since the soil condition in fallow rice paddies after harvest drainage is usually moist but non-waterlogged, it can stimulate N_2O production and inhibit the reduction of N_2O to N_2 in denitrification (Shang et al., 2020). To convert growing-season emissions to annual emissions, a limited number of correction factors are currently available for a few cropping systems, or are restricted for application in specific regions (Pelster et al., 2022). Therefore, it is critical to quantify the contribution of fallow-period N_2O emissions to the annual total emissions at global scale, and to provide reliable correction factors.

The contribution of the fallow period to annual total N_2O emissions varies with management practices, soil properties and climatic conditions. The type of cropping system is an integrated indicator of the specific crops cultivated within a year, management practices and the surrounding environmental conditions. For example, the single rice cropping system, which is generally adopted in humid high-altitude regions, has a longer and cooler fallow period compared to double rice cropping in humid low-altitude regions. In contrast, rice-wheat and maize-wheat systems have the shortest fallow periods in all cropping setups, ranging from two to three months. A recent study revealed that precipitation and temperature are key driving factors for fallow-period N_2O emissions in the US Midwest (Yang et al., 2023). In a previous study, we revealed the role of factors like crop types, annual precipitation, soil pH, and soil organic carbon in determining the difference in N_2O EF caused by the omissions of fallow period

(Shang et al., 2020). However, the global pattern of the contribution of fallow-period N_2O emissions and the associated drivers remain unclear. This is mainly due to the lack of a quantitative model and a fallow calendar for different cropping systems. It hinders our understanding of the importance of fallow-period N_2O emissions and our ability to accurately estimate national and global N_2O emissions in GHG inventories.

To address these gaps, we quantified the ratio of fallow to whole-year emissions (R_{fallow}) using a mixed-effect model that connected crop-specific R_{fallow} variations to climate, soil and agricultural management practices. We conducted our analysis using 360 chamber-based field observations, spanning 53 sites globally. By combining the spatial datasets of the physical areas of multiple cropping systems, crop calendar and crop-specific fertilizer N inputs (including synthetic fertilizers, manure, and crop residues), we compiled datasets of gridded N input and the duration of fallow period for each cropping system. Using the datasets with management and environmental variables, and the model constrained by the global observations, we mapped crop-specific R_{fallow} at the spatial resolution of five-arcminute and identified the key drivers of spatial variations in R_{fallow}. Finally, we converted growing-season N_2O emissions to whole-year emissions at global scale, aiming to reconcile the discrepancies in cropland N_2O emissions estimated by different methodologies.

2 Data and Methods

2.1 Observations for quantifying R_{fallow}

We compiled a global observation dataset consisting of 360 R_{fallow} values from currently available literature databases and online data repositories (Supplementary Text 1). The observed R_{fallow} values were calculated based on fallow and annual N_2O emissions for different single (i.e., legumes, maize, wheat, rice, and others) or double cropping systems (i.e., rice-rice, rice-upland, upland-upland). Triple cropping systems (e.g., rice-rice-rapeseed) are very rare in modern global food production (Waha et al., 2020), and their fallow-period N_2O emission measurements are rather limited. Thus, these systems were excluded from the analysis. Studies with the following measurements were further excluded: (i) experiments conducted in laboratories, pots or greenhouses, (ii) measurements conducted in organic (peaty) soils where N_2O are much higher than those in mineral soils (IPCC, 2006), and (iii) measurements with the use of controlled-release fertilizers, nitrification inhibitors, or urease inhibitors. The full dataset is a combination of data from 57 sites globally and 49 peer-reviewed papers and dissertations, including 71 observations for rice-rice, 25 for rice-upland, 20 for upland-upland systems, 25 for legumes, 49 for maize, 75 for wheat, 60 for rice, and 35 for other single cropping systems (Fig. S1 and Table S1).

For each record, four categories of information were collected: (i) N_2O emissions, (ii) climatic conditions, (iii) soil properties, (iv) management practices, and (v) sampling information. The N_2O emissions for the whole year and fallow period were obtained from the studies identified to calculate the ratios. The fallow period was defined as the period between harvesting crop and sowing or transplanting the next crop. Climatic conditions include mean annual air temperature (MAT) and mean annual precipitation (MAP), fallow-period mean air temperature (FT) and precipitation (FP). Soil properties contain soil organic carbon content (SOC), pH, bulk density (BD), and clay and sand content. Along with climatic conditions, these soil properties influence the substrate availability and soil aeration and determine the rates of microbial processes underlying N_2O emissions (Bouwman et al., 2013; Butterbach-Bahl et al., 2013). Management practices include cropping system type, N fertilizer application rate and fallow duration. These practices are significant due to their known impacts on agroecosystem C and N cycling and fallow period emissions (Cui et al., 2021; Shang et al., 2020). Sampling information include mean sampling interval during fallow period, and whether sampling frequency is intensified at N_2O flux peaks when the mean interval during fallow period is greater than 7 days (Supplementary Text 2 and Fig. S2). Most information was obtained from the original papers; values not reported in the original papers were obtained from climate and soil databases (Supplementary Text 1). The definition and unit of each variable and related information can be found in Supplementary Table S2.

The representativeness of the observations in terms of a per-pixel representation of the relative proportion of interpolation, was assessed according to the method van den Hoogen et al. (2019). To investigate how well our compiled observation dataset spread throughout the full multivariate covariate space (for all soil, climate and management practice-related variables in the model), we performed a principal component analysis (PCA)-based approach. Firstly, we utilised the centring values, scaling values, and eigenvectors to transform the composite image into the same PCA space. Subsequently, we generated convex hulls for each of the bivariate combinations from the first seven principal components, which collectively accounted for over 90% of the sample space variation. Based on the coordinates of these convex hulls, we classified each pixel as falling within or outside of them, that is a per-pixel representation of the relative proportion of interpolation and extrapolation. The relative percentage of interpolation reflects how adequately our dataset captured the multivariate covariate space of the global layers.

2.2 Linear mixed-effect model for R_{fallow}

We developed a linear mixed-effect (LME) model to generate an interpretable regression of R_{fallow} in response to various environmental and management-related factors. The LME is capable of capturing the fixed effects quantified by the key factors and identifying the random effects for N_2O emissions, which can be represented by the sites (Cui et al., 2021). First, to enhance the ability of model to capture the variance, R_{fallow} was converted from the original range of 0 to 1 (11 negative values were excluded) to an infinite range with normal distribution using equation E1, and independent variables were re-scaled using “scale” function in R v.4.2.2.

Second, partial correlation and a generalized boosted regression mode (GBM) were used to determine the key variables for the model. GBM was performed using the “gbm” package in R v.4.2.2. GBM is an ensemble tree-based method that combines multiple weak models to form a single strong model, based on the prior trees, to quantify the relative importance of each variable. Third, the Akaike information criterion (AIC) was implemented by adding variables based on the priority order and the most relevant variables for the LME model were selected to avoid over-fitting (Table S3). Fourth, we checked for interactions among variables. An analysis of variance (ANOVA) test indicated that the model with an interaction between cropping system type and N fertilization rate outperformed other models. Eventually, the LME model included cropping system type, soil pH, N fertilization rate, and fallow duration as fixed-effect terms. Additionally, the model incorporated the site identity in the intercept as a random-effect term (Equation E2). The interaction between the cropping system and N application rate was considered in the LME model through distinguishing slopes corresponding to different cropping systems and N fertilization rates. R_{fallow} for each cropping system was then quantified as follows:

$$R_{fallow\,i} = e^{y_i}/(1 + e^{y_i}), \quad \text{E1}$$

$$y_i = (\alpha + \varphi_i) + (\beta + \theta_i) \cdot Nrate_i + \gamma \cdot pH + \delta \cdot D_i + (1|Site) + \varepsilon_i, \quad \text{E2}$$

where y is the mediator between R_{fallow} and driving variables selected to facilitate the normal distribution of R_{fallow}; i denotes the type of eight cropping systems mentioned above; Nrate is nitrogen (N) fertilizer application rate (kg N ha^{-1}); pH is soil pH; D is the duration of a fallow period in days; Site means the location of the observational field experiments; α, β, γ, δ, φ, and θ are variable coefficients; ε is the residual term. $(\alpha + \varphi_i) + (\beta + \theta_i) \cdot Nrate$ represents the interactive effect between N fertilizer application rate and cropping system, allowing for the eight different cropping systems in our analysis to vary in their response (i.e., slope and intercept) to changes in N application rate; $1|Site$ represents the random-effect term in the mixed-effect model. All the model parameters were quantified using the "lmer" function in the R package "lme4".

The model was trained and tested on a tenfold cross-validation repeated ten times. Cross-validation has been widely used in many studies (Viscarra Rossel et al., 2019; Bo et al., 2022; Malakouti, 2023). The tenfold cross-validation involves splitting all the observations into 10 equal parts, training the model on 9 parts, and testing it on the remaining part. This process is repeated 10 times, with each part used as the test set exactly once. To avoid bias due to subsets randomly divided, we repeated the above steps by 10 times for possible subdivisions. The advantage of cross-validation is that it provides a more reliable estimate of model performance compared to a single train-test split. By averaging the results of different test sets, it reduces the variability of a single partition and provides a more accurate assessment of how the model is likely to perform on unseen data. The coefficients of the model based on 100 trainings were stored for spatial prediction. The performance and robustness of the model were evaluated by comparing simulated and observed R_{fallow} by cropping system, using the 1:1 line, R^2 of fixed effect (R^2c), R^2 of mixed effect (R^2m), slope and root mean square error (RMSE). Additionally, the responses of R_{fallow} to the key variables selected were estimated for each cropping system in the sensitivity tests, with the uncertainty of one standard error using the "sjPlot" package in R. The ranges of the key variables in the sensitivity tests were constrained by those of the observations.

2.3 Global prediction of R_{fallow}

The global patterns of R_{fallow} for each cropping system were simulated using the "predict" function in the LME model at a spatial resolution of 5-arcminutes, which were driven by the duration of the fallow period, the N application rate, and the soil pH. Soil pH was derived directly from the HWSD v1.2 at a resolution of 30-arc-second. Data regarding the spatial distribution of the eight cropping systems, the duration of the fallow period, and the N application rate for each cropping system were specifically compiled for this study.

Physical areas of cropping systems were derived from Waha et al. (2020), which reported multiple attributes including cropping intensity (single, double, or triple), types of crops grown in the system (out of a pool of 26 crops from MIRCA2000 (Monfreda et al., 2008)). Crops without planting and harvesting calendars (e.g., citrus and grapes) were excluded from this study. In the end, 45 out of the initial 70 cropping systems were identified and obtained for this study. The global gridded physical areas for these 45 cropping systems were first resampled from 30´×30´ resolution to a 5´×5´ resolution using the nearest resampling method, then directly summed to obtain the physical area for each of the eight cropping systems. We grouped the double cropping systems into rice-rice, rice-upland, and upland-upland systems, the single cropping systems into legumes, maize, wheat, rice, and the remaining falling under the other cropping system, producing a total of 8 cropping systems. We did not distinguish between rain-fed and irrigated systems.

Crop planting and harvesting dates from Sacks et al. (2010) were used as the reference to establish the duration of the fallow period for each cropping system. We firstly classified each of the obtained 45 cropping system layers as either a single or double cropping. For single cropping systems, the duration of the fallow period in each grid cell was calculated as the interval between the harvesting (H) and planting (P) dates of the corresponding crop, as provided by Sacks et al. (2010) (Equation E3).

$$FDs_{i,j} = \begin{cases} 365 - H_{i,j} + P_i, P_{i,j} < H_{i,j} \\ P_{i,j} - H_{i,j}, \quad P_{i,j} > H_{i,j} \end{cases} \tag{E3}$$

Where $FDs_{i,j}$ represents the duration of the fallow period for cropping system *i* in grid cell *j*; $H_{i,j}$ and $P_{i,j}$ correspond to the harvesting date and planting date, respectively, for crop *i* in grid cell *j*.

For double cropping systems, the duration of the fallow period was calculated as the period without a crop actively growing within a calendar year. For each grid cell, the planting and harvesting dates for both the initial and subsequent crops in the rotation were identified. The duration of the fallow period for each double cropping system was then calculated accordingly by equation E4, as shown below.

$$FDs_{i,j} = \begin{cases} P_{i_2,j} - H_{i_1,j} + 365 - H_{i_2,j} + P_{i_1,j}, \;\; P_{i_1,j} < H_{i_1,j}, P_{i_2,j} < H_{i_2,j} \\ P_{i_2,j} - H_{i_1,j} + P_{i_1,j} - H_{i_2,j}, \;\; P_{i_1,j} < H_{i_1,j}, P_{i_2,j} > H_{i_2,j} \\ P_{i_2,j} - H_{i_1,j} + P_{i_1,j} - H_{i_2,j}, \;\; P_{i_1,j} > H_{i_1,j}, P_{i_2,j} < H_{i_2,j} \end{cases} \tag{E4}$$

Where $FDs_{i,j}$ represents the duration of the fallow period for double cropping system *i* in grid cell *j*; $H_{i_1,j}$, $P_{i_1,j}$, $H_{i_2,j}$, and $P_{i_2,j}$ correspond to the harvesting date and planting date for the first crop i_1 in cropping system *i* in grid cell *j*, harvesting date and planting date for the second crop i_2 in cropping system *i* in grid cell *j*, respectively. Lastly, the average duration of the fallow period for the eight cropping systems was obtained by weighting the physical areas of the different cropping systems.

Crop-specific N application rates per unit of harvested area and total N inputs from Adalibieke et al. (2023) were used to calculate the N application rates per unit of physical area for the eight cropping systems in our study. Firstly, we re-organized the abovementioned physical areas of the 45 cropping systems into 15 crop groups (without accounting for differences in cropping frequency) out of 21 crops from Adalibieke et al. (2023). To address the differences in the physical area reported by Waha et al. (2020) and Adalibieke et al. (2023), missing N application rates for some specific physical areas in 2000 were imputed from nationally averaged N application rates, with the sum of N inputs for a crop and a country kept consistent as the original dataset (Adalibieke et al., 2023). N application rates per physical hectare were calculated for the 45 cropping systems. For a single cropping system, it was set to be the N application rate per harvested hectare of the corresponding crop, while for a double cropping system, the rate was equal to the sum of N application rates per harvested hectare for the corresponding first and second crops. Next, total N application inputs for the eight cropping systems investigated at each grid were aggregated by summing the products of the corresponding physical areas and N application rates from 45 cropping systems.

Lastly, the N application rate per unit of physical area for each cropping system was generated by dividing the total N input by the corresponding physical area. The maximum N application rates were capped at 1,000 and 2,000 kg N ha^{-1} for single and double cropping systems to avoid extremes, respectively.

We conducted 100 simulations of global R_{fallow} with the 100 sets of coefficients from the tenfold cross-validation repeated ten times, and then obtained the global prediction by averaging the predictions from the 100 simulations (Viscarra Rossel et al., 2019). To calculate the weighted R_{fallow} for all cropping systems, we firstly calculated the mediator *y* for each cropping system, and then averaged them based on their corresponding areas to get the weighted *y*. Finally, we transformed the weighted *y* to weighted R_{fallow} according to Equation E1. In this case, we prefer to weight *y* rather than R_{fallow}, because *y* is more sensitive to small differences among cropping systems with its infinite range. For the global prediction of R_{fallow}, their results are quite comparable (Fig. S3) with almost the same mean values (mean ± standard error of the mean: 44.65±0.23% and 44.03±0.24% for weighted R_{fallow}-based and weighted y-based methods respectively).

For the attribution of spatial variation in R_{fallow}, the dominant driver was defined as the factor with the largest absolute value of the partial correlation coefficient (par) in each grid cell, where par between R_{fallow} and predictors is done for 3.75°-by-3.75° moving windows (Beer et al., 2010; Cui et al., 2021; Peng et al., 2014). To identify the dominant driver for all cropping systems, we multiplied the area percentage of each cropping system (i.e., the ratio of area for single rice to the area for all cropping systems) and the par of each factor for that system. Then, the factor with the largest absolute value of par across all cropping systems, was regarded as the most important variable determining the variation of R_{fallow}.

3 Results and Discussion

3.1 Modelling performance and response functions

Soil pH, cropping system type, N application rate and fallow duration were identified as the most important determinants of R_{fallow} than the environmental factors (i.e., soil sand and clay content, BD, SOC, MAP, MAT, FP and FT) included in our analysis (Fig. 1a, Fig. S4 and Table S7). The repeated tenfold cross-validation results indicate that LME model, with the four most important factors as fixed effects and site as a random effect, captured 63% of the observed variation in R_{fallow} (Fig. 1b). The combination of the four key fixed effects, i.e., soil pH, cropping system, N application rate and fallow duration, explained 41% of the observed variation in R_{fallow}. This means that the fixed effect in the model developed explained more variation in R_{fallow} than the random effect did (Supplementary Text 3). The slope between simulated and observed R_{fallow} is 0.73. These results are comparable with those using all the observations for both training and testing (Table S4). The representativeness analysis shows that the observations used for model development covered the vast majority of global variations, with 76% of global pixel values falling within the sampled range of at least 90% of all bands (Fig. S5). Together, the results indicate that our model is effective and robust (Cui et al., 2021;

Philibert et al., 2012). The corresponding means and standard errors of the model coefficients are listed in Table S5.

Among the eight cropping systems included in our analysis, the results show that the single rice system had the largest R_{fallow} at 53±6% (mean ± 95% confidence interval of the mean), followed by double rice-rice (46±7%), single other crops (39±7%), legumes (38±9%), wheat (37±5%), rice-upland (30±8%), upland-upland (21±8%), and single maize cropping systems (16±5%) (Fig. 1c). Single-cropping systems generally showed greater R_{fallow} than double-cropping systems. Rice-dominated cropping systems (i.e., single rice and double rice-rice) exhibited larger R_{fallow} than the other systems.

Cropping system type is an integrated indicator representing local management practices and environmental conditions. Its influence can be largely attributed to factors such as MAT, MAP, and fallow duration, which collectively captured 50–99% of the variations observed for all cropping systems (Table S6). For instance, the single rice system in temperate and subtropical climate areas had the longest fallow duration (223 days for single rice compared to 159 days for the remainder systems). The associated moisture soil conditions after harvest drainage in this extended fallow period are favourable for N_2O emissions (Shang et al., 2020). In contrast, upland-upland and rice-upland cropping systems, which have the shortest fallow durations (62 and 114 days on average, respectively) and relatively lower soil moisture levels, which limits N_2O emissions during the fallow period.

Sensitivity tests indicated that R_{fallow} was negatively correlated with soil pH (Fig. 1d) but positively correlated with the fallow duration (Fig. 1f). Specifically, R_{fallow} in double rice-rice, rice-upland, and wheat cropping systems responded more strongly to variations in soil pH and fallow duration than other cropping systems, while the single maize appeared at the lower end of all response curves (Fig. 1d and f). The results indicate that R_{fallow} for rice-related cropping systems was more sensitive to N application rate than the other cropping systems, especially at N application rates <400 kg N ha^{-1} (Fig. 1e). This is probably because rice-related cropping systems had higher initial R_{fallow} (without N fertilization) than other cropping systems, due to the moist soil conditions during fallow period promoting N_2O emissions. Fertilizer N additions further increased growing-season N_2O emissions, which contributed the most to annual emissions, thereby reducing R_{fallow}. Together, these results suggest that the underestimation of cropland N_2O emission inventory based on EF methodologies, due to the omission of fallow-period N_2O emissions, can be potentially exaggerated for rice-related systems, especially at low levels of N fertilizer inputs.

3.2 Spatial pattern of R_{fallow}

It is estimated that global average value of R_{fallow} (i.e., weighted by areas of global cropping systems and expressed as a percentage) was 44.0%, with a 95% confidence interval (CI) ranging from 14.5 to 74.6% (Table 1). The highest R_{fallow} was 56.6% (28.3–81.1%) for single wheat cropping, followed by 52.3% (14.1–79.7%) for rice, 48.8% (27.0–71.6%) for legumes, and 44.9% (23.6–68.7%) for others, 34.6% (8.5–

65.4%) for maize, 26.2% (1.3–61.5%) for double rice-rice, 12.4% (1.9–30.2%) for rice-upland crops, and 10.5% (1.6–24.1%) for upland-upland crops (Table 1). The hotspots of high R_{fallow} (>60%) estimated were concentrated in northern high-altitude areas, the Amazon Plain, and Southeast Asia (e.g., Myanmar, Thailand and Laos), while low R_{fallow} (<13%) areas were mainly located in southern high-altitude areas (e.g., Southern Africa, America and Australia), the North China Plain, Mexico and the Southwestern U.S. The areas with high R_{fallow} were dominated by single wheat or rice-related cropping systems, those with low R_{fallow} were mostly covered by other upland crops (Sacks et al., 2010; Waha et al., 2020).

We found high R_{fallow} was concentrated in northern high-altitude areas. These areas generally have lower soil pH and more areas of single cropping systems (e.g., wheat, maize and other crops) (Fig. S6). Based on partial correlation of observations, lower soil pH is significantly related to greater R_{fallow} ($r=-0.36$, $p<0.001$, Table S7). Additionally, pH was strongly and negatively related to simulated R_{fallow} across all cropping systems at global scale (Fig. S7), and was identified as the dominant driver of simulated R_{fallow} over other factors in major high-altitude areas (Fig. 3). Single cropping system in northern high-altitude areas generally have longer fallow period and greater R_{fallow} than double cropping systems.

The results indicate that cropping systems showed distinctive spatial variations in R_{fallow} (Fig. 2b-i). The R_{fallow} estimated for double rice-upland and upland-upland crops (mean ± standard error of the mean: 12.4±0.2 and 10.5±0.1%, respectively) were only a quarter of the R_{fallow} observed for other cropping systems (46.4±0.3%), especially in regions such as the North China Plain, Northeastern China, the Indus Plain, Turkey, and Mexico. In contrast, R_{fallow} for single rice and wheat systems (52.3±0.3 and 56.6 ±0.2%, respectively) were significantly greater than the average of all other systems (39.8±0.3%), with hotspots mainly in regions with tropical and sub-tropical croplands (e.g., Southeastern Asia and Amazon Plain) for single rice, and North high-altitude areas for single wheat. The intrinsic variation in R_{fallow} for these cropping systems can also been found in the observations included in our dataset (Fig. 1c). Single legumes, maize and other systems showed similar spatial variations in R_{fallow} as the area-weighted averages of all systems (Fig. 2a).

3.3 Attribution of the spatial variation in R_{fallow}

Soil pH was identified as the most important driver of spatial variation in R_{fallow} in 72% of the total global cropping area (Fig. 3a). For all cropping systems other than single rice, soil pH was the most important driver in most (>=59%) of their individual global cropping area (Fig. 3b-i). These results likely reflect that low soil pH inhibit the activity of N_2O reductase in denitrification, and reduce the precursor concentration of N_2O formation (i.e., NH_2OH and NO_2^-) in nitrification, thereby stimulating N_2O emissions (Barton et al., 2013; Qin et al., 2014; Russenes et al., 2016; Wang et al., 2021). Consistent with these findings, low soil pH values are associated with greater fallow-period N_2O emissions across the observations included in our dataset (Correlation coefficient=-0.31, p<0.001), leading to the increasing R_{fallow} values with decreasing soil pH. This is probably because lower temperature during the fallow period (e.g., winter season) further inhibits the N_2O reductase activity (Qin et al., 2014). Additionally, lower pH levels are correlated with more precipitation in fallow periods in our dataset (Correlation coefficient=-0.1, $p<0.05$). High precipitation rates may stimulate fallow-period N_2O emissions when low soil water content is the limiting factor for N_2O emissions especially in arid areas (Shang et al., 2020). Since about 50% of global arable soils are acidic, liming has been suggested as a potential practice to increase crop yield (Dai et al., 2017; Wang et al., 2021). In this case, soil liming can decrease the contribution of fallow-period to whole-year N_2O emissions in severely acidic area (pH<5.5) concentrated in Eastern US, Northern Germany and Poland, Southern China, and Southeastern Brazil (Wang et al., 2021), and hence influence the growing-season to whole-year N_2O correction factors for these areas.

Fallow duration was identified as the most important driver for R_{fallow} in single rice cropping systems and the second most important factor in most other single cropping systems accounting for 20–34% of the variations in their cropping areas, especially in North America, Northern South America, and Northern China (Fig. 3e-i). A longer fallow period directly results in more N_2O emissions during this fallow period, confirmed by the positive relationships between duration and R_{fallow} across our dataset (Fig. 1f). Compared to double cropping systems, single cropping systems generally have a longer and more variable fallow period that is constrained by local climates. For example, single rice systems have a longer fallow period (1–2 months more) in Northeastern compared to Southern China. These single rice systems in Southern China are usually transformed from double rice systems due to labour shortage (Han et al., 2022), although the light, temperature and rainfall there are favourable for double rice growth. In contrast, the double cropping systems, such as maize-wheat and rice-wheat in Turkey, Northern and Eastern China, generally have a much shorter fallow period, ranging from two to three months. This relatively short fallow period likely explains the negligible effect of fallow duration on the spatial variation in R_{fallow} for double cropping systems (Fig. 3b-d).

The results indicate N application rate was the most important driver in 11–32% of global cropping areas for both double cropping systems and single rice and maize systems (Fig. 3). R_{fallow} estimated generally decreases with increased N application rates (Fig. 1e). This is because fertilizer-induced N_2O emissions mostly occurred during the crop growing seasons when crops need intensive N fertilizer inputs, with limited fertilizer N residues for N_2O emissions during the fallow seasons. MAT was identified as a key factor only in limited areas for double upland crops. However, it emerged as the dominant driver for the variation weighted by cropping systems in Africa, South America, and Southeast Asia.

3.4 Implications for updating N_2O emission inventories

We converted N_2O emissions during the growing season to cover the whole-year emissions (Table 2), based on the estimated area-weighted R_{fallow}, the growing-season dominated default EFs from the IPCC Tier 1 method and our high-resolution cropping-system-specific N application rate developed in this study. Estimated global fertilizer

N-induced cropland N_2O emissions in 2000 substantially increased from 1.0 to 2.1 Tg N, implying a global R_{fallow} of ~53%. Emission hotspots were located in several countries such as China, France, Germany, the U.S. and the U.K. (Fig. S8). Accordingly, the EF more than doubled from 0.9% (based on IPCC Tier1 defaults of 0.4% for paddy rice and 1.0% for upland crops) to 1.9% (0.6% for paddy rice and 2.1% for upland crops). High adjusted EFs (i.e., >2%) were concentrated in regions like Brazil, Middle Africa, Southeast Asia and high-altitude regions in Europe (Fig. 4a). The adjusted global EF is more than twice as large as those from EF-based models based on growing-season N_2O observations (Table 2), and is consistent with results from an ensemble of process-based models (1.8, 1.2–2.3%, Tian et al., 2020) and a recent top-down inversion model (2.3%, Thompson et al., 2019). The process-based models considered the legacy effect from historical soil N accumulation (Tian et al., 2019, 2020), which is the main source of N_2O emissions during the fallow period without fertilization. Since the inversion model estimates EFs based on observed changes in atmospheric N_2O concentrations, it accounts for both direct and indirect emissions. Indirect emissions were not included in our study but account for about one-third of total cropland N_2O emissions (Harris et al., 2022). Comparing our findings with the IPCC Tier1 defaults, significant increases in EFs were found in Russia, Myanmar and some areas dominated with acidic soils and single cropping systems (e.g., wheat and maize) (Fig. 4b), while the increase was trivial in East India and Pakistan, probably due to the vast expansion of double cropping systems (e.g., rice-upland crops and upland-upland crops) with shorter fallow durations (Sacks et al., 2010; Waha et al., 2020), alongside the prevalence of alkaline soils in Pakistan. The consistency between the estimates of our corrected EF-based model and other independent models strongly suggests that most of the discrepancies between the models were caused by the omission of fallow-period N_2O emissions. Our findings are also in alignment with previous findings that the global EF for cropland N_2O emissions is significantly higher than the IPCC default (Thompson et al., 2019; Tian et al., 2020). Thus, to improve estimates of N_2O inventories, we suggest that fallow-period N_2O emissions should be included in the EF-based models. For the datasets reporting growing-season N_2O emissions only, without considering fallow-period emissions, they should not be further considered in the calculation of IPCC N_2O EFs. IPCC should update the relevant EFs.

3.5 Limitations and future perspective

Although our approach considers the influences of various important factors, some limitations should be noted. First, to improve our estimation for various cropping systems (e.g., double rice-rice, single rice, and single wheat systems), more field measurements of fallow-period N_2O emissions are needed for double rice-upland crops, upland-upland crops, and single legume systems. About 81% of the observations are based on averaged or intensified sampling intervals of no more than 7 days during fallow period (Supplementary Text 2), however, future field studies should ensure frequent fallow-period measurements especially during N_2O peak-flux periods (e.g., spring thawing and tillage) to improve data reliability. Second, site-specific microscale variables were less recorded and their effects on local N_2O emissions were not fully quantified due to limited understanding of the mechanisms of microbial N_2O productions (Cui et al., 2021; Kravchenko et al., 2017). These can lead to some uncertainties in the global simulation, however, the fixed effect in the model developed explained more variation in R_{fallow} than the random effect (represented by site identity) did. Other uncertainties come from recently introduced or highly-localized practices in fallow periods, such as winter cover cropping, tillage and continuous flooding for water storage in hilly rice paddies. Although tillage showed an insignificant impact on growing-season or whole-year N_2O emissions based on meta-analyses (van Kessel et al., 2013; Shang et al., 2021), it can increase fallow-period N_2O emissions due to the favourable soil aeration and water content for N_2O productions in field experiments (Mosier et al., 2006; Zhang et al., 2016). Similarly, the return of crop residue or green manure can increase fallow-period N_2O emissions in the fields through providing more C and N substrates for nitrification and denitrification processes (Liu et al., 2015; Li et al., 2021). As indicated in the field studies above, fallow tillage and return of crop residue or green manure generally have a more positive impact on fallow-period over growing-season N_2O emissions, and hence increase the value of R_{fallow}. However, these effects may vary with time (e.g., beginning or end of fallow period) and type of practice (e.g., straw mulching or incorporation, and residue composition), which needs more information and deserves further investigation. Constrained by the availability of crop-specific spatial data, the global R_{fallow} was estimated using the spatial distribution of cropping systems in 2000. Some single cropping systems have evolved to double cropping systems and vice versa over the last 20 years (Han et al., 2022), which might slightly affect the contribution of fallow period emission in recent years. However, our model is not restricted to specific years and sites, and it can be applied universally based on essential factors such as soil properties and management practices, regardless of time and space.

N_2O emissions in fallow period have been ignored when calculating the whole-year emissions for decades, even though this will lead to the underestimation of N_2O emission inventories. One major objective of our study was to understand the degree to which cropland N_2O emissions have been underestimated in the EF-based models. Here we demonstrate that the inclusion of fallow-period N_2O emissions is crucial for compiling accurate cropland whole-year N_2O emission inventories. In particular, single wheat and other single cropping systems dominate most global fallow emissions, contributing up to 89% of their whole-year emissions. Overall, our estimates of the global average EF more than doubled from 0.9 to 1.9% when the emissions during the fallow periods were considered, with variations in R_{fallow} mainly driven by soil pH and management practices (i.e., cropping system type, N fertilizer application rate, and fallow duration). Current EF-based models systemically underestimate N_2O fluxes without the corresponding adjustment for the fallow period. Additionally, process-based models are barely capable of calibrating and validating against the measurements of fallow-period N_2O emissions, due to the limitation of available fallow emission measurements. Hence, a sharing platform of global fallow-period N_2O emission measurements is needed to gather more comprehensive data on fallow-period N_2O emissions. Further research is required to check if historical trends and future projections of national cropland N_2O emissions would be impacted by the inclusion of fallow period. Additionally, research on potential mitigation practices specific to reducing N_2O emissions during fallow periods is needed, especially for single or rice-related cropping systems. Overall, our study extends our understanding of the contribution of fallow-period N_2O emissions – the global magnitude, spatial variation, and their environmental and anthropogenic drivers. We hope our approach can be used to improve future N_2O inventories and to inform mitigation efforts to reduce cropland N_2O emissions.

Acknowledgements

This study was supported by the Youth Innovation Program of Chinese Academy of Agricultural Sciences (No. Y2023QC02), the National Natural Science Foundation of China (42225102, 42301059, 32172129, 42207378), the National Key Research and Development Program of China (2021YFD1700801, 2022YFD2300400), Technology Research System-Green manure (Grant No. CARS-22-G-16).

Appendix A. Supplementary data

Supplementary information related to this article can be found online, including Supplementary Texts 1 to 3, Tables S1 to S7, and Figures S1 to S8.

Author contributions

Feng Zhou: Conceptualization, Writing - review & editing, Funding acquisition, Project administration. Ziyin Shang: Conceptualization, Methodology, Investigation, Formal analysis, Visualization, Writing – original draft, Funding acquisition. Xiaoqing Cui: Methodology, Visualization, Writing – original draft. Matthias Kuhnert, Mohamed Abdalla, Jiafa Luo, Kees Jan van Groenigen, Weijian Zhang, Zhenwei Song, Yu Jiang, and Pete Smith: Resources, Conceptualization, Writing - review & editing.

Conflicts of interest

The authors declare no conflicts of interest.

References

Adalibieke, W., Cui X.Q., Cai H.W., You L.Z., F, Z. (2023). Global crop-specific nitrogen fertilization dataset in 1961-2020. *Scientific Data*, 10, 617. https://doi.org/10.1038/s41597-023-02526-z.

Barton, L., Gleeson, D. B., Maccarone, L. D., Zúñiga, L. P., & Murphy, D. V. (2013). Is liming soil a strategy for mitigating nitrous oxide emissions from semi-arid soils? *Soil Biology and Biochemistry*, 62, 28–35. https://doi.org/10.1016/j.soilbio.2013.02.014

Beer, C., Reichstein, M., Tomelleri, E., Ciais, P., Jung, M., Carvalhais, N., Rödenbeck, C., Arain, M. A., Baldocchi, D., Bonan, G. B., Bondeau, A., Cescatti, A., Lasslop, G., Lindroth, A., Lomas, M., Luyssaert, S., Margolis, H., Oleson, K. W., Roupsard, O., . . . Papale, D. (2010). Terrestrial Gross Carbon Dioxide Uptake: Global Distribution and Covariation with Climate. *Science*, 329(5993), 834-838. https://doi.org/10.1126/science.1184984

Bouwman, A.F., Beusen, A.H.W., Griffioen, J., Van Groenigen, J.W., Hefting, M.M., Oenema, O., Van Puijenbroek, P., Seitzinger, S., Slomp, C.P., Stehfest, E. (2013). Global trends and uncertainties in terrestrial denitrification and N_2O emissions. *Philosophical Transactions of the Royal Society B-Biological Sciences*, 368. https://doi.org/10.1098/rstb.2013.0112.

Bo, Y., Jägermeyr, J., Yin, Z., Jiang, Y., Xu, J. Z., Liang, H., & Zhou, F. (2022). Global benefits of non-continuous flooding to reduce greenhouse gases and irrigation water use without rice yield penalty. *Global Change Biology*, 28(11), 3636-3650. https://doi.org/10.1111/gcb.16132

Butterbach-Bahl, K., Baggs, E.M., Dannenmann, M., Kiese, R., Zechmeister-Boltenstern, S. (2013). Nitrous oxide emissions from soils: how well do we understand the processes and their controls? *Philosophical Transactions of the Royal Society B-Biological Sciences*, 368. https://doi.org/10.1098/rstb.2013.0122.

Crippa, M., Guizzardi, D., Solazzo, E., Muntean, M., Schaaf, E., Monforti-Ferrario, F., Banja, M., Olivier, J.G.J., Grassi, G., Rossi, S., Vignati, E. (2021). GHG emissions of all world countries - 2021 Report. *Publications Office of the European Union*. https://doi.org/10.2760/173513.

Cui, X.Q., Zhou, F., Ciais, P., Davidson, E.A., Tubiello, F.N., Niu, X.Y., Ju, X.T., Canadell, J.G., Bouwman, A.F., Jackson, R.B., Mueller, N.D., Zheng, X.H., Kanter, D.R., Tian, H.Q., Adalibieke, W., Bo, Y., Wang, Q.H., Zhan, X.Y., Zhu, D.Q. (2021). Global mapping of crop-specific emission factors highlights hotspots of nitrous oxide mitigation. *Nature Food*, 2, 886-893. https://doi.org/10.1038/s43016-021-00384-9.

Dai, Z., Zhang, X., Tang, C., Muhammad, N., Wu, J., Brookes, P. C., & Xu, J. (2017). Potential role of biochars in decreasing soil acidification – A critical review. *Science of the Total Environment*, 581–582, 601–611. https://doi.org/10.1016/j.scitotenv.2016.12.169

Deng, Z., Ciais, P., Tzompa-Sosa, Z.A., Saunois, M., Qiu, C., Tan, C., Sun, T., Ke, P., Cui, Y., Tanaka, K., Lin, X., Thompson, R.L., Tian, H., Yao, Y., Huang, Y., Lauerwald, R., Jain, A.K., Xu, X., Bastos, A., Sitch, S., Palmer, P.I., Lauvaux, T., d'Aspremont, A., Giron, C., Benoit, A., Poulter, B., Chang, J., Petrescu, A.M.R., Davis, S.J., Liu, Z., Grassi, G., Albergel, C., Tubiello, F.N., Perugini, L., Peters, W., Chevallier, F. (2022). Comparing national greenhouse gas budgets reported in UNFCCC inventories against atmospheric inversions. *Earth System Science Data*, 14, 1639-1675. https://doi.org/10.5194/essd-14-1639-2022.

Ekwunife, K.C., Madramootoo, C.A., Abbasi, N.A. (2022). Assessing the impacts of tillage, cover crops, nitrification, and urease inhibitors on nitrous oxide emissions over winter and early spring. *Biology and Fertility of Soils*, 58, 195-206. https://doi.org/10.1007/s00374-021-01605-w.

FAO Food and Agricultural Organization of the United Nations. FAOSTAT data. Retrieved June 18, 2018, from http://www.fao.org/faostat/en/#data/RFN (Fertilizers by Nutrient); http://www.fao.org/faostat/en/#data/EMN (Live-stock Manure); http://www.fao.org/faostat/en/#data/GA (Crop Residues); http://www.fao.org/faostat/en/#data/GT (Emissions-Agriculture).

Han, J.C., Zhang, Z., Luo, Y.C., Cao, J., Zhang, L.L., Zhuang, H.M., Cheng, F., Zhang, J., Tao, F.L. (2022). Annual paddy rice planting area and cropping intensity datasets and their dynamics in the Asian monsoon region from 2000 to 2020. *Agricultural Systems*, 200. https://doi.org/10.1016/j.agsy.2022.103437.

Harris, E., Yu, L., Wang, Y.P., Mohn, J., Henne, S., Bai, E., Barthel, M., Bauters, M., Boeckx, P., Dorich, C., Farrell, M., Krummel, P.B., Loh, Z.M., Reichstein, M., Six, J., Steinbacher, M., Wells, N.S., Bahn, M., Rayner, P. (2022). Warming and redistribution of nitrogen inputs drive an increase in terrestrial nitrous oxide emission factor. *Nature Communications*, 13. https://doi.org/10.1038/s41467-022-32001-z.

Li, J., Wang, S., Shi, Y. L., Zhang, L. L., & Wu, Z. J. (2021). Do Fallow Season Cover Crops Increase N_2O or CH_4 Emission from Paddy Soils in the Mono-Rice Cropping System? *Agronomy-Basel*, 11(2). https://doi.org/ARTN 19910.3390/agronomy11020199

Liu, W., Hussain, S., Wu, L. S., Qin, Z. G., Li, X. K., Lu, J. W., Khan, F., Cao, W. D., & Geng, M. J. (2016). Greenhouse gas emissions, soil quality, and crop productivity from a mono-rice cultivation system as influenced by fallow season straw management. *Environmental Science and Pollution Research*, 23(1), 315-328. https://doi.org/10.1007/s11356-015-5227-7

Malakouti, S. M. (2023). Improving the prediction of wind speed and power production of SCADA system with ensemble method and 10-fold cross-validation. *Case Studies in Chemical and Environmental Engineering*, 8, 100351. https://doi.org/10.1016/j.cscee.2023.100351

Mosier, A. R., Halvorson, A. D., Reule, C. A., & Liu, X. J. J. (2006). Net global warming potential and greenhouse gas intensity in irrigated cropping systems in northeastern Colorado. *Journal of Environmental Quality*, 35(4), 1584-1598. https://doi.org/10.2134/jeq2005.0232

Monfreda, C., Ramankutty, N., & Foley, J. A. (2008). Farming the planet: 2. Geographic distribution of crop areas, yields, physiological types, and net primary production in the year 2000. *Global Biogeochemical Cycles*, 22(1). https://doi.org/Artn Gb102210.1029/2007gb002947

Kravchenko, A. N., Toosi, E. R., Guber, A. K., Ostrom, N. E., Yu, J., Azeem, K., Rivers, M. L., & Robertson, G. P. (2017). Hotspots of soil N_2O emission enhanced through water absorption by plant residue. *Nature Geoscience*, 10(7), 496-+. https://doi.org/10.1038/Ngeo2963

Pelster, D.E., Thiagarajan, A., Liang, C., Chantigny, M.H., Wagner-Riddle, C., Congreves, K., Lemke, R., Glenn, A., Tenuta, M., Hernandez-Ramirez, G., Bittman, S., Hunt, D., Owens, J., MacDonald, D. (2022). Ratio of non-growing season to growing season N_2O emissions in Canadian croplands: an update to national inventory methodology. *Canadian Journal of Soil Science*. https://doi.org/10.1139/cjss-2022-0101.

Peng, S. S., Piao, S. L., Ciais, P., Myneni, R. B., Chen, A. P., Chevallier, F., Dolman, A. J., Janssens, I. A., Peñuelas, J., Zhang, G. X., Vicca, S., Wan, S. Q., Wang, S. P., & Zeng, H. (2013). Asymmetric effects of daytime and night-time warming on Northern Hemisphere vegetation. *Nature*, 501(7465), 88-+. https://doi.org/10.1038/nature12434

Philibert, A., Loyce, C., & Makowski, D. (2012). Quantifying Uncertainties in N_2O Emission Due to N Fertilizer Application in Cultivated Areas. Plos One, 7(11). https://doi.org/ARTN e5095010.1371/journal.pone.0050950

Qin, S.P., Yuan, H.J., Hu, C.S., Oenema, O., Zhang, Y.M., Li, X.X. (2014). Determination of potential N_2O-reductase activity in soil. *Soil Biology & Biochemistry*, 70, 205-210. https://doi.org/10.1016/j.soilbio.2013.12.027.

Ravishankara, A., Daniel, J.S., Portmann, R.W. (2009). Nitrous oxide (N_2O): the dominant ozone-depleting substance emitted in the 21st century. *Science*, 326, 123-125. https://doi.org/10.1126/science.1176985

Russenes, A.L., Korsaeth, A., Bakken, L.R., Dorsch, P. (2016). Spatial variation in soil pH controls off-season N_2O emission in an agricultural soil. *Soil Biology & Biochemistry*, 99, 36-46. https://doi.org/10.1016/j.soilbio.2016.04.019.

Sacks, W.J., Deryng, D., Foley, J.A., Ramankutty, N. (2010). Crop planting dates: an analysis of global patterns. *Global Ecology and Biogeography*, 19, 607-620. https://doi.org/10.1111/j.1466-8238.2010.00551.x.

Shang, Z.Y., Abdalla, M., Kuhnert, M., Albanito, F., Zhou, F., Xia, L.L., Smith, P. (2020). Measurement of N_2O emissions over the whole year is necessary for estimating reliable emission factors. *Environmental Pollution*, 259. https://doi.org/10.1016/j.envpol.2019.113864.

Shang, Z. Y., Abdalla, M., Xia, L. L., Zhou, F., Sun, W. J., & Smith, P. (2021). Can cropland management practices lower net greenhouse emissions without compromising yield? *Global Change Biology*, 27(19), 4657-4670. https://doi.org/10.1111/gcb.15796

Thompson, R.L., Lassaletta, L., Patra, P.K., Wilson, C., Wells, K.C., Gressent, A., Koffi, E.N., Chipperfield, M.P., Winiwarter, W., Davidson, E.A., Tian, H., Canadell, J.G. (2019). Acceleration of global N_2O emissions seen from two

decades of atmospheric inversion. *Nature Climate Change*, 9, 993-+. https://doi.org/10.1038/s41558-019-0613-7.
Tian, H.Q., Xu, R.T., Canadell, J.G., Thompson, R.L., Winiwarter, W., Suntharalingam, P., Davidson, E.A., Ciais, P., Jackson, R.B., Janssens-Maenhout, G., Prather, M.J., Regnier, P., Pan, N.Q., Pan, S.F., Peters, G.P., Shi, H., Tubiello, F.N., Zaehle, S., Zhou, F., Arneth, A., Battaglia, G., Berthet, S., Bopp, L., Bouwman, A.F., Buitenhuis, E.T., Chang, J.F., Chipperfield, M.P., Dangal, S.R.S., Dlugokencky, E., Elkins, J.W., Eyre, B.D., Fu, B.J., Hall, B., Ito, A., Joos, F., Krummel, P.B., Landolfi, A., Laruelle, G.G., Lauerwald, R., Li, W., Lienert, S., Maavara, T., MacLeod, M., Millet, D.B., Olin, S., Patra, P.K., Prinn, R.G., Raymond, P.A., Ruiz, D.J., van der Werf, G.R., Vuichard, N., Wang, J.J., Weiss, R.F., Wells, K.C., Wilson, C., Yang, J., Yao, Y.Z. (2020). A comprehensive quantification of global nitrous oxide sources and sinks. *Nature*, 586, 248-256. https://doi.org/10.1038/s41586-020-2780-0.
Tian, H.Q., Yang, J., Xu, R.T., Lu, C.Q., Canadell, J.G., Davidson, E.A., Jackson, R.B., Arneth, A., Chang, J.F., Ciais, P., Gerber, S., Ito, A., Joos, F., Lienert, S., Messina, P., Olin, S., Pan, S.F., Peng, C.H., Saikawa, E., Thompson, R.L., Vuichard, N., Winiwarter, W., Zaehle, S., Zhang, B.W. (2019). Global soil nitrous oxide emissions since the preindustrial era estimated by an ensemble of terrestrial biosphere models: Magnitude, attribution, and uncertainty. *Global Change Biology*, 25, 640-659. https://doi.org/10.1111/gcb.14514.
van den Hoogen, J., Geisen, S., Routh, D., Ferris, H., Traunspurger, W., Wardle, D. A., de Goede, R. G. M., Adams, B. J., Ahmad, W., Andriuzzi, W. S., Bardgett, R. D., Bonkowski, M., Campos-Herrera, R., Cares, J. E., Caruso, T., Caixeta, L. D., Chen, X. Y., Costa, S. R., Creamer, R., . . . Crowther, T. W. (2019). Soil nematode abundance and functional group composition at a global scale. *Nature*, 572(7768), 194-+. https://doi.org/10.1038/s41586-019-1418-6
van Kessel, C., Venterea, R., Six, J., Adviento-Borbe, M. A., Linquist, B., & van Groenigen, K. J. (2013). Climate, duration, and N placement determine N_2O emissions in reduced tillage systems: a meta-analysis. *Global Change Biology*, 19(1), 33-44. https://doi.org/10.1111/j.1365-2486.2012.02779.x
Viscarra Rossel, R. A., Lee, J., Behrens, T., Luo, Z., Baldock, J., & Richards, A. (2019). Continental-scale soil carbon composition and vulnerability modulated by regional environmental controls. *Nature geoscience*, 12(7), 547-552. https://doi.org/10.1038/s41561-019-0373-z
Waha, K., Dietrich, J.P., Portmann, F.T., Siebert, S., Thornton, P.K., Bondeau, A., Herrero, M. (2020). Multiple cropping systems of the world and the potential for increasing cropping intensity. *Global Environmental Change-Human and Policy Dimensions*, 64. https://doi.org/10.1016/j.gloenvcha.2020.102131.
Wang, Q., Zhou, F., Shang, Z., Ciais, P., Winiwarter, W., Jackson, R.B., Tubiello, F.N., Janssens-Maenhout, G., Tian, H., Cui, X., Canadell, J.G., Piao, S., Tao, S. (2020). Data-driven estimates of global nitrous oxide emissions from croplands. *National Science Review*, 7, 441-452. https://doi.org/10.1093/nsr/nwz087.

Wang, Y., Yao, Z. S., Zhan, Y., Zheng, X. H., Zhou, M. H., Yan, G. X., Wang, L., Werner, C., & Butterbach-Bahl, K. (2021). Potential benefits of liming to acid soils on climate change mitigation and food security. Global Change Biology, 27(12), 2807-2821. https://doi.org/10.1111/gcb.15607

Winiwarter, W., Hoglund-Isaksson, L., Klimont, Z., Schoepp, W., Amann, M. (2018). Technical opportunities to reduce global anthropogenic emissions of nitrous oxide. *Environmental Research Letters,* 13. https://doi.org/10.1088/1748-9326/aa9ec9.

Yang, Y.F., Liu, L.C., Zhou, W., Guan, K.Y., Tang, J.Y., Kim, T., Grant, R.F., Peng, B., Zhu, P., Li, Z.Y., Griffis, T.J., Jin, Z.N. (2023). Distinct driving mechanisms of non-growing season N_2O emissions call for spatial-specific mitigation strategies in the US Midwest. *Agricultural and Forest Meteorology*, 335. https://doi.org/10.1016/j.agrformet.2023.109457.

Zhang, G. B., Yu, H. Y., Fan, X. F., Yang, Y. T., Ma, J., & Xu, H. (2016). Drainage and tillage practices in the winter fallow season mitigate CH_4 and N_2O emissions from a double-rice field in China. *Atmospheric Chemistry and Physics*, 16(18), 11853-11866. https://doi.org/10.5194/acp-16-11853-2016

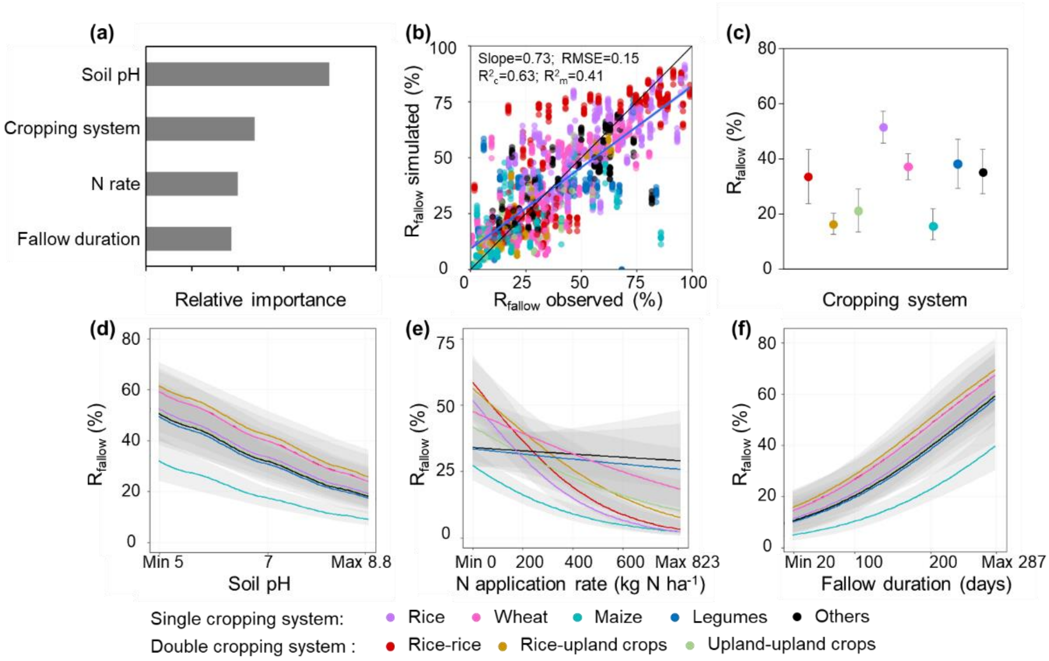

Fig. 1 Relative importance of selected variables (a), model performance (b) and the sensitivity of variable (e-f) for R_{fallow}. The four most important variables (i.e., soil pH, cropping system type, N application rate and fallow duration) were identified by partial correlation and generalized boosted regression mode, and selected in the mixed-effect model based on model AIC. The model was evaluated by R^2 of fixed effect (R^2_c), R^2 of mixed effect (R^2_m) and root mean square error (RMSE) based on a repeated tenfold cross-validation. The mean and error bar of 95% confidence interval were generated by bootstrapping resampling. The shade of sensitivity curve represents one standard error. Color indicates cropping system type for a whole year.

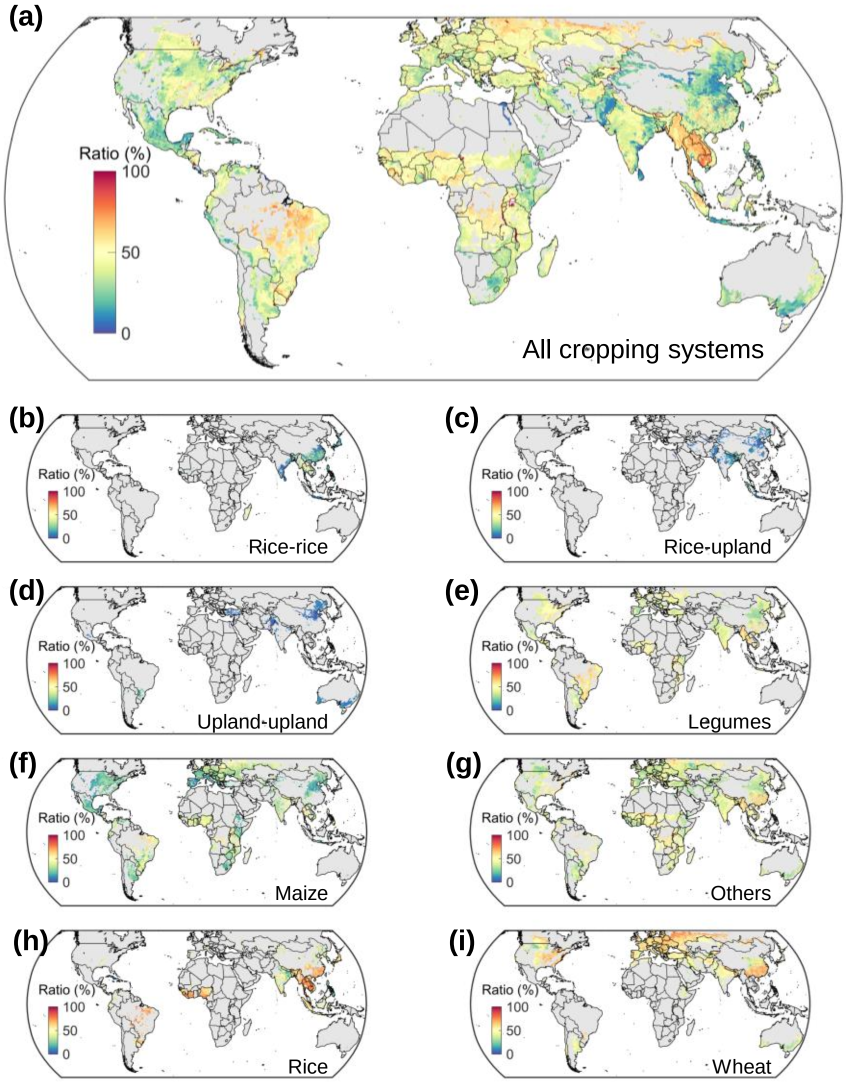

Fig. 2 Global patterns of R_{fallow}. (a) ratios weighted by areas of different cropping systems, including the double (rice-rice (b), rice-upland crops (c) and upland-upland crops (d)) and single (legumes (e), maize (f), others (g), rice (h) and wheat (i)). Ratios were predicted with a linear mixed-effect model. Values are shown only where the proportion of harvested area within the grid cell is greater than 0.5%. Map lines delineate study areas and do not necessarily depict accepted national boundaries.

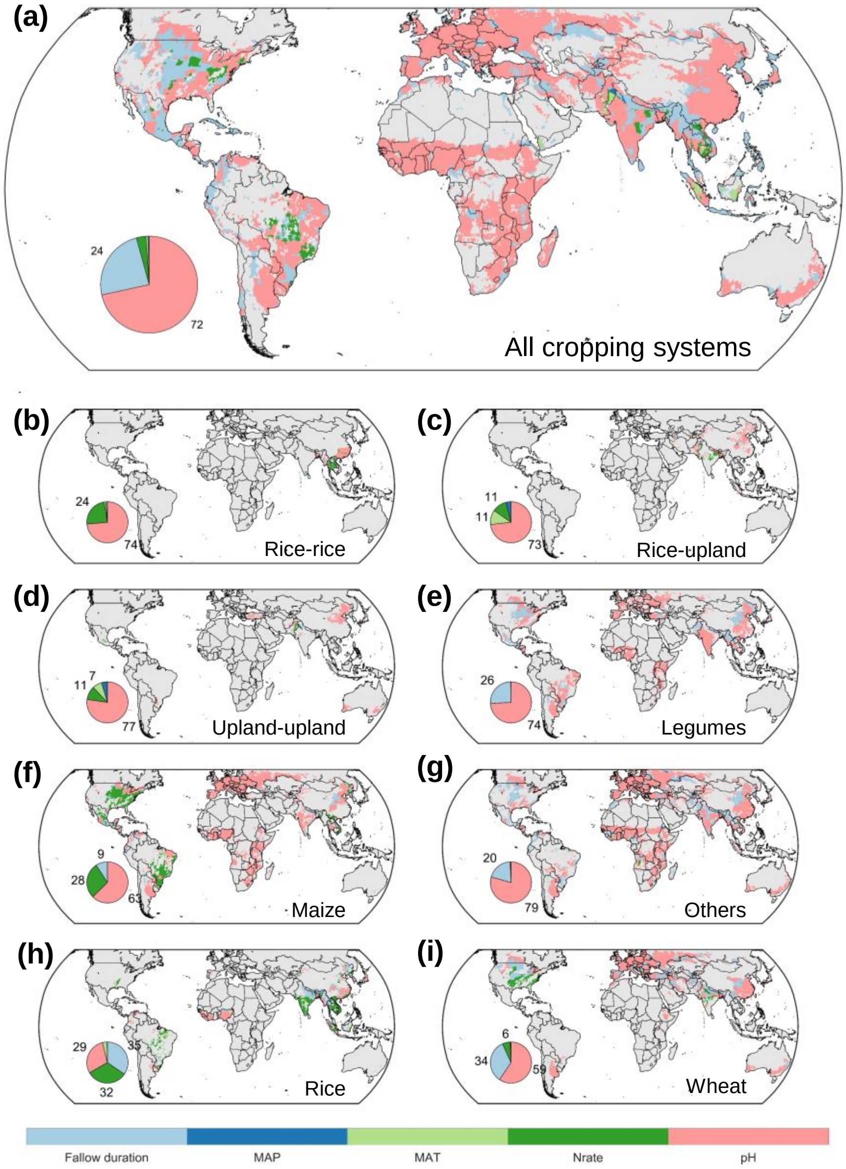

Fig. 3 Distribution of dominant drivers regulating variation in R_{fallow}. (a) ratios weighted by areas of different cropping systems, including the double (rice-rice (b), rice-upland crops (c) and upland-upland crops (d)) and single (legumes (e), maize (f), others (g), rice (h) and wheat (i)). The dominant driver is defined as the factor with the largest absolute value of the partial correlation coefficient (par) in each grid cell, where par between R_{fallow} and predictors is done for 3.75°-by-3.75° moving windows. Significant correlations ($p < 0.05$) are shown. Values are shown only where the

proportion of harvested area within the grid cell is greater than 0.5%. The inset pie plots represent the ratio (%) of harvested areas for which R_{fallow} variation is regulated by the dominant drivers. MAP: mean annual precipitation; MAT: mean annual temperature; Nrate: N application rate. Map lines delineate study areas and do not necessarily depict accepted national boundaries.

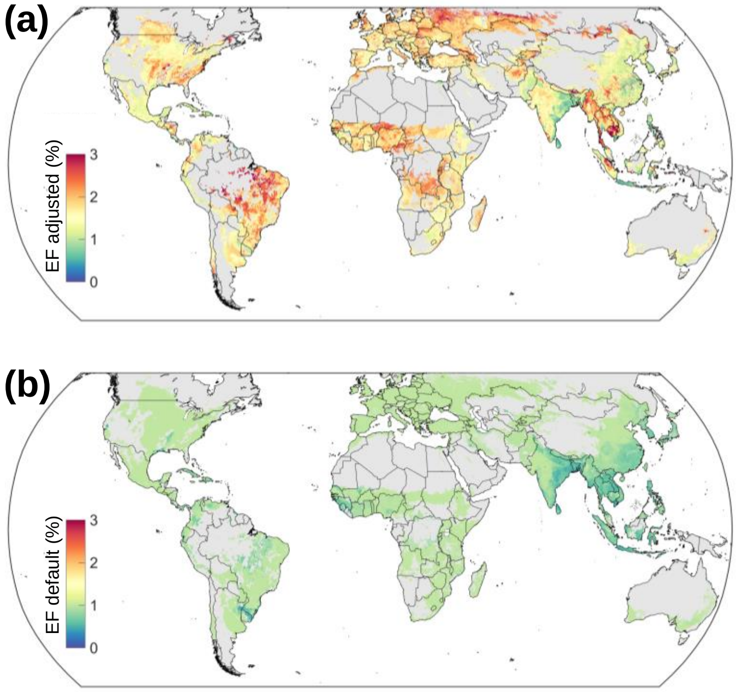

Fig. 4 Spatial variation of cropland N_2O EF estimated in this study (a) and based on IPCC tier 1 EF defaults (b). The R_{fallow} used was the area-weighted of all cropping systems. Map lines delineate study areas and do not necessarily depict accepted national boundaries.

Table 1 Mean and 95% confidence interval (CI) for the stimulated R_{fallow} by cropping system.

Category	Cropping system	Mean (%)	95% CI (%)
Single	Wheat	56.5	28.3–81.1
	Rice	52.3	14.1–79.7
	Legumes	48.8	27.0–71.6
	Others	44.9	23.6–68.7
	Maize	34.6	8.5–65.4
Double	Rice-rice	26.2	1.3–61.5
	Rice-upland crops	12.4	1.9–30.2
	Upland-upland crops	10.5	1.6–24.1
Global		44.0	14.5–74.6

Table 2 Cropland fertilizer-induced N_2O emissions and emission factor from main approaches.

Methodology	Year	Emission (Tg N)	EF(%)	Citation
This study	2000	2.1	1.9	This study
Emission factor-based model	2000	1.0–1.4	0.9–1.0	
FAO[a]	2000	1.3	0.9	FAOSTAT, 2022
EDGAR[a]	2000	1.5	0.9	Crippa et al., 2021
GAINS[a]	2000	1.4	0.9	Winiwarter et al., 2018
SRNM	2000	1.1	1.0	Wang et al., 2020
LME	2000	1.0	0.9	Cui et al., 2021
Process-based model ensemble	2000s	2 (1.3–3.4)[b]	1.8 (1.2–2.3)	Tian et al., 2020
Atmospheric inversion[c]	1998–2016	-	2.3±0.6	Thompson et al., 2019

[a] FAOSTAT and GAINS were normalized by removing the contribution from synthetic fertilizers applied to pasture; the EDGAR version 4.3.2 by excluding the contributions from synthetic fertilizers applied to pasture and soil mineralization.

[b] The emission from the ensemble of process-based models includes cropland and pasture N_2O emissions.

[c] The inversion model includes direct and indirect N_2O emissions.

Figure Legends

Fig. 1 Relative importance of selected variables (a), model performance (b) and the sensitivity of variable (e-f) for R_{fallow}. The four most important variables (i.e., soil pH, cropping system type, N application rate and fallow duration) were identified by partial correlation and generalized boosted regression mode, and selected in the mixed-effect model based on model AIC. The model was evaluated by R^2 of fixed effect (R^2_c), R^2 of mixed effect (R^2_m) and root mean square error (RMSE) based on a repeated tenfold cross-validation. The mean and error bar of 95% confidence interval were generated by bootstrapping resampling. The shade of sensitivity curve represents one standard error. Color indicates cropping system type for a whole year.

Fig. 2 Global patterns of R_{fallow}. (a) ratios weighted by areas of different cropping systems, including the double (rice-rice (b), rice-upland crops (c) and upland-upland crops (d)) and single (legumes (e), maize (f), others (g), rice (h) and wheat (i)). Ratios were predicted with a linear mixed-effect model. Values are shown only where the proportion of harvested area within the grid cell is greater than 0.5%. Map lines delineate study areas and do not necessarily depict accepted national boundaries.

Fig. 3 Distribution of dominant drivers regulating variation in R_{fallow}. (a) ratios weighted by areas of different cropping systems, including the double (rice-rice (b), rice-upland crops (c) and upland-upland crops (d)) and single (legumes (e), maize (f), others (g), rice (h) and wheat (i)). The dominant driver is defined as the factor with the largest absolute value of the partial correlation coefficient (par) in each grid cell, where par between R_{fallow} and predictors is done for 3.75°-by-3.75° moving windows. Significant correlations ($p < 0.05$) are shown. Values are shown only where the proportion of harvested area within the grid cell is greater than 0.5%. The inset pie plots represent the ratio (%) of harvested areas for which R_{fallow} variation is regulated by the dominant drivers. MAP: mean annual precipitation; MAT: mean annual temperature; Nrate: N application rate. Map lines delineate study areas and do not necessarily depict accepted national boundaries.

Fig. 4 Spatial variation of cropland N_2O EF estimated in this study (a) and based on IPCC tier 1 EF defaults (b). The R_{fallow} used was the area-weighted of all cropping systems. Map lines delineate study areas and do not necessarily depict accepted national boundaries.